4420 *J. Phys. Chem. A* **2004,** *108,* 4420−4427

Vibrational Overtone Spectroscopy of Jet-Cooled Aminophenols as a Probe for Rotational Isomers

Timothy W. Robinson and Henrik G. Kjaergaard*

Department of Chemistry, University of Otago, P.O. Box 56, Dunedin, New Zealand

Shun-ichi Ishiuchi, Minako Shinozaki, and Masaaki Fujii

Chemical Resources Laboratory, Tokyo Institute of Technology, PRESTO/JST, 4259 Nagatsuta,
Yokohama, 226-8053, Japan

Received: November 24, 2003; In Final Form: March 11, 2004

Nonresonant ionization detected (NID) spectroscopy has been used to record the OH-, NH-, and CH-stretching vibrational overtone spectra of *o*-, *m*-, and *p*-aminophenol (aminohydroxybenzene; hydroxyaniline) in the collision-free environment of a supersonic jet. The OH-, NH-, and CH-stretching fundamental vibrations of jet-cooled *o*- and *m*-aminophenol have also been studied by NID and infrared-depletion techniques. We use an anharmonic oscillator local mode model, with one oscillator for each OH, NH, and CH bond, to calculate the frequencies and intensities of the stretching transitions and facilitate the assignment of the measured vibrational spectra. In the case of *m*-aminophenol, the presence of two rotational isomers is clearly demonstrated in the higher vibrational overtone spectra. For *o*-aminophenol, we find that one rotational isomer dominates, and the possible existence of a second is discussed. Electronic structure calculations are used to determine and explain the relative energies of the various rotational isomers. Our results show that vibrational overtone spectroscopy combined with jet-cooled conditions is a powerful technique for distinguishing between rotational isomers.

Introduction

The gas-phase spectroscopy of small aromatic molecules can provide valuable information on larger and more flexible molecules of biological importance.[1,2] The aminophenol molecule is a prototype for studying the interactions of more complicated aromatic amines and alcohols, such as the structurally related amino acid tyrosine and the neurotransmitter dopamine. Aminophenol is a particularly appealing molecule for spectroscopic study because it exhibits both structural and rotational isomerism, determined by the relative positions and conformations of the amino and hydroxyl substituents. In *m*-aminophenol, rotational isomers exist that are energetically distinct due to different steric and electronic interactions, and for *o*-aminophenol the close proximity of the substituents provides potential for the formation of NH···O or OH···N intramolecular hydrogen bonds.

Microwave spectroscopy has long been used to study rotational isomers. In recent times, a combination of molecular beams or supersonic jets with tunable lasers operating in the ultraviolet has enabled rotational isomers to be distinguished by their respective electronic transitions.[3−6] Vibrational overtone spectroscopy is another technique that is sensitive to subtle changes in molecular conformation;[7] however, the broadness of bands in room temperature overtone spectra has so far limited the observation of rotational isomers. The width of vibrational bands can be reduced substantially by recording the spectra in the low-temperature environment of supersonic jet expansions.[8] One such technique is nonresonant ionization detected (NID) infrared (IR) and near-infrared (NIR) spectroscopy, which has recently been used to record the overtone spectra of jet-cooled phenol[9] and aniline.[10]

Previous studies have shown that individual vibrational overtone transitions of nonequivalent bonds are consistently resolved when the bond lengths differ by as little as 1 mÅ.[7,11] Recently, we reported the NID-IR/NIR vibrational spectrum of jet-cooled catechol (1,2-dihydroxybenzene) up to the third OH-stretching overtone ($\Delta v_{OH} = 4$).[12] The catechol molecule has a weak (ca. 2.5 kcal mol^{-1}) intramolecular hydrogen bond, and the spectrum showed two peaks in each OH-stretching region, with the peak at lower wavenumber corresponding to the hydrogen-bonded OH-stretching oscillator. The separation of the two OH-stretching transitions increased from 57 cm^{-1} in the fundamental region to 273 cm^{-1} at $\Delta v_{OH} = 4$.

For *m*-aminophenol, cis and trans (or syn and anti) rotational isomers have been identified via dispersed fluorescence and laser induced fluorescence spectroscopy.[13,14] The cis and trans conformers differ only in the position of the hydroxy hydrogen atom, and the effect that this subtle difference in structure has on the OH-stretching vibrational frequencies should be visible in the vibrational overtone spectra.

Recently, the OH- and NH-stretching fundamental vibrations of jet-cooled *p*-aminophenol were measured by IR-depletion (IR-dip) spectroscopy.[15,16] Prior to this, the vibrational spectroscopy of aminophenols had been limited primarily to solid and solution phase studies, from which limited information on rotational isomers can be extracted.[17−19]

In this paper we present the XH-stretching (where X = C, N, and O) overtone spectra of *o*-, *m*-, and *p*-aminophenol recorded in a supersonic jet expansion. The vapor pressures of

---

* Corresponding author. E-mail: henrik@alkali.otago.ac.nz. Fax: 64-3-479-7906. Phone: 64-3-479-5378.

10.1021/jp037577y CCC: $27.50

the aminophenols are low and for this reason we have used the sensitive NID technique. In addition to the NID spectra, we present the IR-dip spectrum of *o*-aminophenol recorded in the XH-stretching fundamental region.

We use the harmonically coupled anharmonic oscillator (HCAO) local mode model[20,21] combined with ab initio calculated dipole moment functions (DMFs) to calculate the frequencies and intensities of the XH-stretching fundamental and overtone transitions,[22,23] and use these calculations to facilitate the assignment of our spectra. Electronic structure calculations are used to determine the relative energies of the rotational isomers, and the origin of the energy differences is investigated by using natural bond orbital analysis. We compare our present results to those obtained for the structurally related molecules phenol[9,24,25] and aniline.[10,26,27]

Experimental Section

The nonresonant ionization detected (NID) infrared−near-infrared (IR-NIR) spectra of jet-cooled *o*-, *m*-, and *p*-aminophenol (Wako 98%) were measured in a supersonic jet. The aminophenol samples were purified by vacuum sublimation prior to use. The NID spectroscopic technique has been described in detail previously.[9,25] Briefly, NID is an IR-NIR/UV double resonance technique that selectively ionizes a vibrationally excited molecule by nonresonant 2-photon excitation. The necessary UV radiation is generated by a frequency doubled dye laser (Sirah: Cobra Stretch), which is pumped by the second harmonic of a Nd^{3+}:YAG laser (Spectra Physics: INDI). The UV radiation used was 310, 330, and 327.5 nm for the measurement of *o*-, *m*-, and *p*-aminophenol, respectively. Tunable IR radiation from 2600 to 5600 cm^{-1} was obtained by the differential mixing technique between the fundamental or second harmonics of the YAG laser and the dye laser output. Tunable NIR radiation was obtained with an OPO laser (Spectra Physics: MOPO-HF/PRO250) in the 5600−11400 cm^{-1} range, and with a dye laser (Lumonics HD-500) in the 13200−14200 cm^{-1} range, using the LDS751 and LD700 dyes. The line width of the IR/NIR lasers was less than 0.1 cm^{-1} in all regions.

The UV and IR-NIR beams were coaxially (from opposite directions) and simultaneously introduced into the vacuum chamber and focused where they crossed the supersonic jet. The cations generated by UV excitation were pushed into a detector chamber where they were detected by a channel multiplier (Murata Ceratron). The ion signal was amplified by a preamplifier (EG&G PARC 115) and was integrated by a digital boxcar (EG&G PARC 4420/4422). The integrated signal was recorded as a function of the IR-NIR laser wavelength.

Mixtures of aminophenol vapor and He gas were expanded into the vacuum chamber through a solenoid valve. The melting points of *o*-, *m*-, and *p*-aminophenol are 174, 124, and 188 °C, respectively, and the *m*- and *p*-aminophenol samples were heated to 80 °C, and *o*-aminophenol to 70 °C, to increase the vapor pressures. The samples were seeded in 3 atm of He gas, which produced a jet temperature of about 10 K. Spectral bands in the NID spectra were deconvoluted into Lorentzian peaks with a linear baseline with the Igor Pro (v. 4.02) curve-fitting program.

IR-dip spectroscopy is also an IR-UV double resonance technique and the experimental setup is similar to that used for the NID experiment. In IR-dip spectroscopy, the frequency of the UV laser is tuned to the S_1-S_0 electronic transition of a specific species and the resonance-enhanced multiphoton ionization (REMPI) signal from the UV radiation is monitored. The signal intensity is proportional to the population of the specific species in the vibrational ground state of the S_0 electronic state. The IR laser is introduced about 50 ns before the UV radiation and is scanned. If the frequency of the IR laser is resonant with any of the vibrational levels the population of the ground state decreases and correspondingly the REMPI signal decreases. Therefore, the vibrational transitions of a specific species in its electronic ground state can be observed as a depletion (dip) in the spectrum.[28]

TABLE 1: Calculated OH- and NH-Stretching Local Mode Parameters (in cm^{-1})[a]

	o-aminophenol (trans)		*m*-aminophenol				*p*-aminophenol	
			cis		trans			
mode	$\tilde{\omega}$	$\tilde{\omega}x$	$\tilde{\omega}$	$\tilde{\omega}x$	$\tilde{\omega}$	$\tilde{\omega}x$	$\tilde{\omega}$	$\tilde{\omega}x$
OH[b]	3833.9	84.05	3825.5	84.32	3827.4	84.13	3831.5	84.32
NH_t[c]	3629.7	80.96	3628.0	81.68	3631.5	81.51	3615.2	81.99
NH_a[c]	3634.2	81.68	3629.7	81.54	3632.6	81.50	3614.5	81.98

[a] Calculated with the B3LYP/6-311++G(2d,2p) method. [b] Scaled with 0.9959 and 0.8723 for $\tilde{\omega}$ and $\tilde{\omega}x$, respectively. [c] Scaled with 1.0018 and 1.0049 for $\tilde{\omega}$ and $\tilde{\omega}x$, respectively.

Theory and Calculations

The dimensionless oscillator strength f of a transition from the ground vibrational state g to an excited vibrational state e is given by[22,29]

$$f = 4.702 \times 10^{-7}[\text{cm D}^{-2}]\tilde{\nu}_{eg}|\vec{\mu}_{eg}|^2 \qquad (1)$$

where $\tilde{\nu}_{eg}$ is the transition frequency in cm^{-1} and $\vec{\mu}_{eg} = \langle e|\vec{\mu}|g\rangle$ is the transition dipole moment in Debye (D).

In XH-stretching (where X = C, N, and O) overtone spectra, coupling to lower frequency modes can to a good approximation be neglected. The OH bond and CH bonds are described as isolated local modes,[23] each approximated by a Morse oscillator with the Hamiltonian

$$(H - E_{|0\rangle})/hc = v\tilde{\omega} - (v^2 + v)\tilde{\omega}x \qquad (2)$$

where $E_{|0\rangle}$ is the energy of the vibrational ground state and $\tilde{\omega}$ and $\tilde{\omega}x$ are the local mode frequency and anharmonicity, respectively. Coupling between the two NH-stretching modes in the amino group is included by use of the harmonically coupled anharmonic oscillator (HCAO) local mode model.[20,30]

The local mode parameters are obtained from ab initio calculated anharmonic potential energy curves along the internal stretching coordinates.[31,32] The potential energy curves are calculated at nine points by stretching each bond by ±0.2 Å in steps of 0.05 Å. We have scaled the calculated local mode parameters $\tilde{\omega}$ and $\tilde{\omega}x$ with appropriate scaling factors that were determined by comparison of calculated and experimental $\tilde{\omega}$ and $\tilde{\omega}x$ values for phenol (OH bond),[9] aniline (NH),[27] and benzene (CH),[33] molecules for which experimental local mode parameters have been determined. The calculated local mode parameters for the OH- and NH-stretching oscillators, and the corresponding scaling factors used, are given in Table 1. The coupling parameter for the NH_2 group is obtained from the splitting between the symmetric and asymmetric NH-stretching fundamental transitions.[22]

The dipole moment function (DMF) required in eq 1 is approximated as a series expansion in the internal displacement coordinates, with expansion coefficients determined from density functional theory calculations at the equilibrium geometry and at geometries in which the bond is displaced from equilibrium. Two-dimensional DMFs are calculated for the NH_2 groups. We

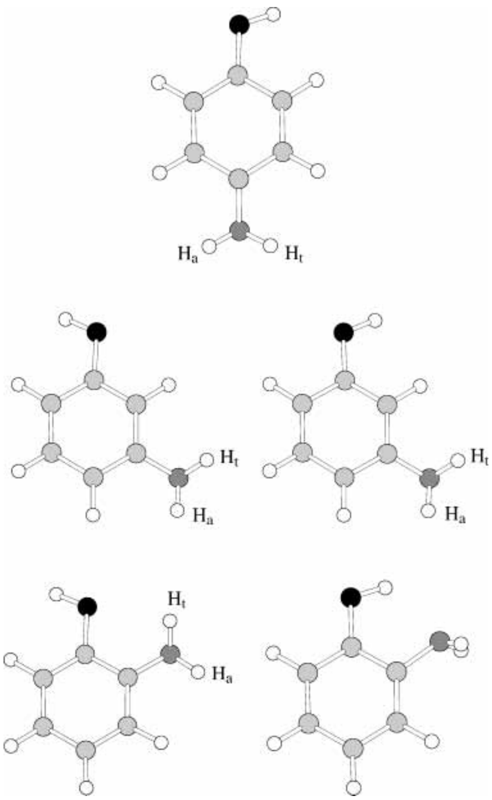

Figure 1. B3LYP/6-311++G(2d,2p) optimized structures of *o*- (bottom), *m*-, (middle), and *p*-aminophenol (top). For *o*- and *m*-aminophenol, trans (left) and cis (right) rotational isomers are shown. The *cis*-*o*-aminophenol structure has C_s symmetry.

have calculated the DMFs with the B3LYP hybrid functional and a 6-311++G(2d,2p) basis set. In previous studies we have shown that the B3LYP/6-311++G(2d,2p) method is successful at predicting vibrational frequencies and intensities of XH-stretching overtones, while being computationally feasible for use with a molecule the size of aminophenol.[12,27]

We have used the B3LYP densities in natural bond orbital (NBO) analyses[34] of the cis and trans conformers of *o*-aminophenol to examine the principal delocalization interactions and explain their relative stabilities. NBO analysis involves the transformation of the wave function into a localized form corresponding to maximum occupancy in one-atom (lone pair) and two-atom (bond) regions of the molecule. The set of high-occupancy NBOs represents the natural Lewis structure of the molecule, and delocalization of electron density from these bonding or lone pair NBOs into the antibonding NBOs corresponds to irreducible departures from the Lewis structure. The strength of the stabilization interactions is estimated by second-order perturbation theory, or by recalculating the total energy after deleting specific orbitals and their associated delocalization interactions.[34]

The electronic structure calculations were performed with the Gaussian 98 package.[35] All geometries were optimized with the "tight" convergence criterion without any constraints on the optimization. The dipole moments were calculated as the analytical derivative of the energy, and "tight" convergence was used in the self-consistent field. The B3LYP calculations used the Becke weighting scheme for numerical integration.

Results and Discussion

The B3LYP/6-311++G(2d,2p) optimized structures of *o*-, *m*-, and *p*-aminophenol are shown in Figure 1, and the calculated OH and NH bond lengths are presented in Table 2. Only one conformer is possible for *p*-aminophenol, while for *m*-aminophenol and *o*-aminophenol we have considered the possibility of two rotational isomers, cis and trans, which refer to the direction that the hydroxyl group points relative to the amino group. For all aminophenol isomers, with the exception of *cis*-*o*-aminophenol, the NH$_2$ group adopts an aniline-like geometry, where the nitrogen is situated a few degrees below the ring plane and the amino hydrogens sit above the ring. This arrangement of the amino group allows for the maximum resonance interaction between the nitrogen lone pair and the aromatic ring (vide infra). The NH bonds are nonequivalent and we have labeled the amino hydrogen that points toward the hydroxyl group "H$_t$" and the one that faces away "H$_a$". In all aminophenol structures, the OH group is situated in the plane of the ring, similar to what is observed for the phenol molecule.[9]

TABLE 2: Calculated OH and NH Bond Lengths (in Å)[a]

bond	*o*-aminophenol (trans)	*m*-aminophenol cis	*m*-aminophenol trans	*p*-amino-phenol	phenol	aniline
OH	0.9609	0.9614	0.9614	0.9610	0.9615	
NH$_t$	1.0077	1.0073	1.0072	1.0083		1.0074
NH$_a$	1.0069	1.0073	1.0071	1.0083		1.0074

[a] Calculated with the B3LYP/6-311++G(2d,2p) method.

The cis and trans conformers of *m*-aminophenol are both true minima on the B3LYP/6-311++G(2d,2p) potential energy surface (no imaginary frequencies). The distance between the two substituents is sufficient that the interactions are weak and the NH$_2$ group adopts a position very similar to that of the NH$_2$ group in aniline. In the *cis*-*m*-aminophenol conformer the NH$_2$ group is rotated slightly (2°) about the CN bond away from the OH group. The trans conformer has a B3LYP/6-311++G(2d,2p) calculated energy, including zero-point vibrational energy correction, that is 0.44 kcal mol^{-1} lower than that of the cis conformer. At our experimental mixing temperature of 80 °C this corresponds to a trans to cis ratio of about 2:1 and we would expect to observe both rotational isomers in the NID experiment.

In the case of *o*-aminophenol, the B3LYP/6-311++G(2d,2p) calculations predict that only the trans conformer is a true minimum. The *trans*-*o*-aminophenol molecule exhibits a slight lengthening of the NH$_t$ bond, and a slight contraction of the NH$_a$ bond, compared to the aniline molecule. These bond length changes suggest the existence of a very weak NH···O hydrogen-bonding interaction. The changes in bond lengths are accompanied by a 3° rotation of the CN bond so that the H$_t$ atom is somewhat closer to the O atom. In *cis*-*o*-aminophenol, the calculated OH bond length (0.9729 Å) is significantly longer compared to the other structures, as a result of relatively strong OH···N intramolecular hydrogen bonding. The B3LYP/6-311++G(2d,2p) calculated harmonic frequencies and IR intensities for the five structures shown in Figure 1 are given as Supporting Information in Table 1S.

In Figure 2 we show the NID overview spectra of jet-cooled *o*-, *m*-, and *p*-aminophenol in the 5600−11500 and 13200−14200 cm^{-1} regions. The overview spectra clearly show the dominance of the pure local mode stretching vibrations. The OH-stretching vibrations are the dominant transitions, and are observed up to the third vibrational overtone ($\Delta v_{OH} = 4$). Each of the aminophenols has four nonequivalent CH bonds, and the $\Delta v_{CH} = 2$ transitions are observed as broad, weak bands in the 6000 cm^{-1} region. The CH-stretching oscillators are less anharmonic than the OH- and NH-stretching ones and it is not surprising that the CH-stretching transitions cannot be clearly observed at higher overtones. The broadness of the CH-

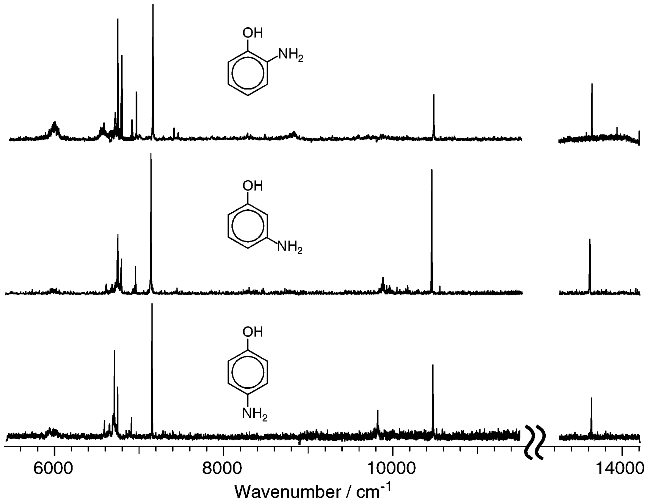

Figure 2. NID overview spectra of jet-cooled *o*-, *m*-, and *p*-aminophenol.

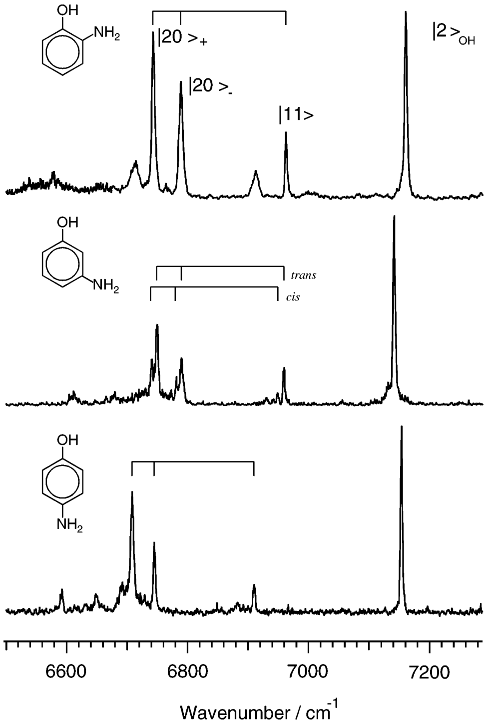

Figure 3. NID spectra of jet-cooled *o*-, *m*-, and *p*-aminophenol in the $\Delta v_{\mathrm{OH}} = 2$ and $\Delta v_{\mathrm{NH}} = 2$ regions.

stretching bands suggests fast intramolecular vibrational relaxation and a larger density of effective dark states.

OH-Stretching Vibrations. The detailed spectra of the regions corresponding to $\Delta v_{\mathrm{OH}} = 2$, 3, and 4 are shown in Figures 3, 4, and 5, respectively. The observed band positions are compared to values calculated with our anharmonic oscillator model in Table 3, in which we also compare to the previous results for phenol.[9] The NID-IR spectrum of *p*-aminophenol in the fundamental region has been reported previously, and for completeness we have recorded the NID-IR fundamental spectra of *o*- and *m*-aminophenol and show these in Figure 6.

There is very good agreement between the observed and calculated band positions. The largest deviation in the calculated frequencies for the aminophenols is about 10 cm^{-1}, which is particularly satisfying considering that calculated local mode parameters have been used. Within each vibrational manifold the OH-stretching wavenumber increases in the order *m*- < *p*- < *o*-aminophenol, which is in agreement with the calculated transition frequencies and the relative bond lengths shown in Table 2. The OH-stretching transitions in *m*-aminophenol are located at similar energies to those of phenol, while those in *o*- and *p*-aminophenol are at higher energy.

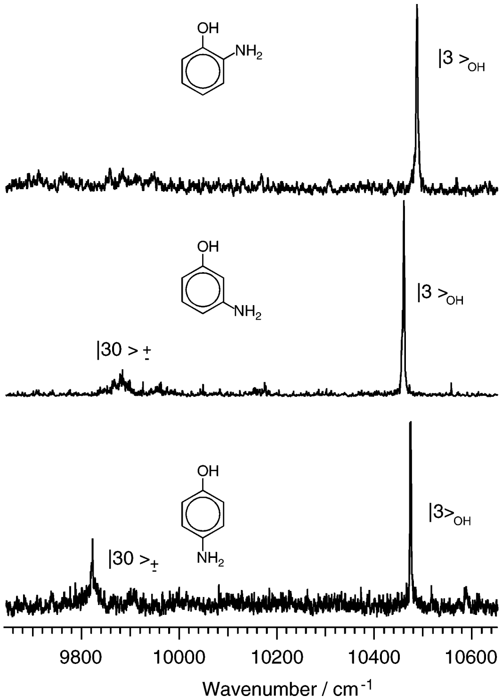

Figure 4. NID spectra of jet-cooled *o*-, *m*-, and *p*-aminophenol in the $\Delta v_{\mathrm{OH}} = 3$ and $\Delta v_{\mathrm{NH}} = 3$ regions.

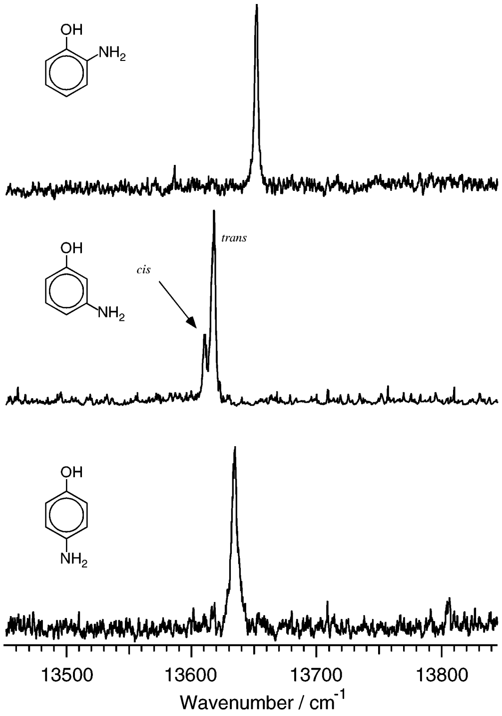

Figure 5. NID spectra of jet-cooled *o*-, *m*-, and *p*-aminophenol in the $\Delta v_{\mathrm{OH}} = 4$ region.

In Figure 7 we show the OH-stretching overtone transitions of the cis and trans conformers of *m*-aminophenol, where we have set the dominant peak, assigned to the trans conformer, at zero on the wavenumber axis. The separation between the trans and cis transitions increases with increasing vibrational overtone, in excellent agreement with the calculated frequencies shown

TABLE 3: Observed and Calculated OH−Stretching Frequencies (in cm^{-1})

	o-aminophenol (trans)		*m*-aminophenol				*p*-aminophenol		phenol	
			cis		trans					
v	obsd	calcd[a]	obsd	calcd[a]	obsd	calcd[a]	obsd	calcd[a]	obsd[b]	calcd[c]
1	3666	3666	3658	3657	3658	3659	3663[d]	3663	3656	3656
2	7161	7163	7140	7145	7142	7150	7154	7157	7143	7143
3	10488	10493	10457	10465	10461	10472	10475	10483	10461	10461
4	13652	13654	13611	13616	13618	13627	13635	13640	13612	13610

[a] Calculated with the local mode parameters in Table 2. [b] Taken from ref 9. [c] Calculated with experimental local mode parameters. [d] Taken from ref 16. Reference 15 reported a value of 3660 cm^{-1}.

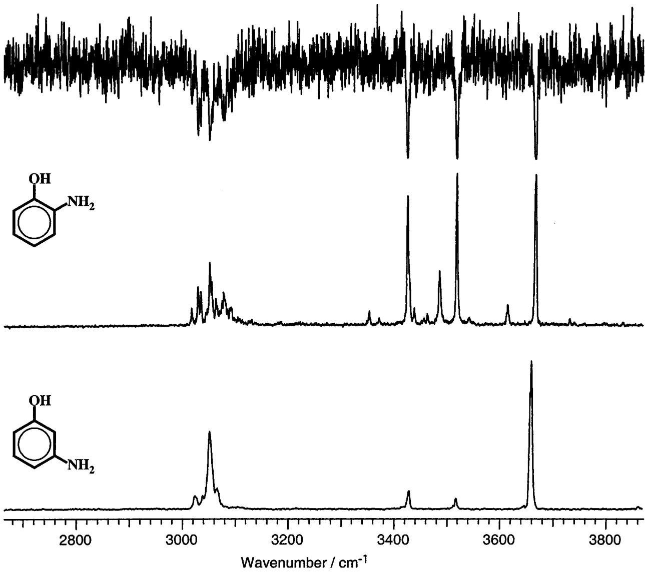

Figure 6. NID-IR spectra of jet-cooled *o*- and *m*-aminophenol and IR-dip spectrum of jet-cooled *o*-aminophenol (top).

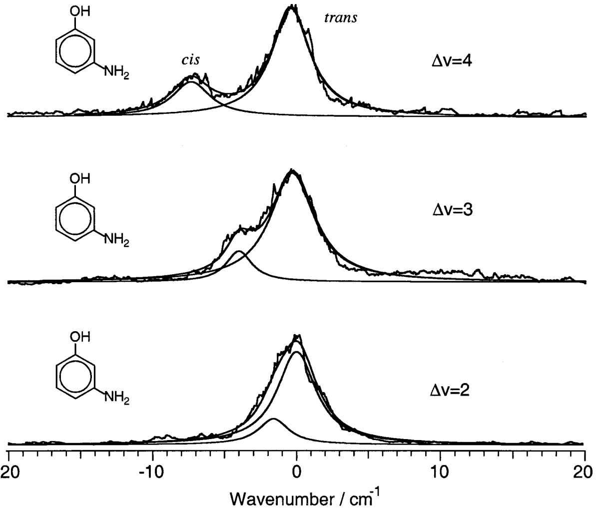

Figure 7. NID spectra of jet-cooled *m*-aminophenol in the $\Delta v_{\mathrm{OH}} = 2$, 3, and 4 regions. The position of the peak assigned to the trans conformer has been set to zero at each overtone.

in Table 3. At the highest overtone recorded, $\Delta v_{\mathrm{OH}} = 4$, the cis and trans OH-stretching transitions are well-resolved. However, even at jet-cooled conditions, resolution of the two conformers is not possible in the fundamental and first overtone regions, such is the subtlety of the structural difference between the two conformers. The OH bonds have calculated bond lengths that differ by only 0.02 mÅ, and calculated local mode frequencies that differ by only 2 cm^{-1}.

In the $\Delta v_{\mathrm{OH}} = 4$ region, the observed relative intensity of the trans and cis peaks is estimated to be about 4:1 from deconvolution of the spectrum. A combination of our calculated oscillator strengths and measured transition intensities makes it possible to determine experimentally the relative energies of the two conformers. The two conformers have very similar calculated oscillator strengths for their respective $\Delta v_{\mathrm{OH}} = 4$ transitions and thus the observed intensity ratio should be directly proportional to the relative abundance of the two conformers. The abundance ratio is about 2:1 calculated from the B3LYP/6-311++G(2d,2p) energy difference of 150 cm^{-1} and a mixing temperature of 80 °C. On the basis of our experimental results we would suggest that the cis−trans energy difference is somewhat larger than the B3LYP calculated value.

Ruoff et al.[36] studied the relaxation of conformers in supersonic expansions seeded with He, Ne, Ar, and Kr gases and found that no relaxation was caused by the light carrier gas He, and furthermore, that molecules with barriers to internal rotation of greater than 400 cm^{-1} did not relax significantly in any of the carriers. We calculate a barrier to rotation in *m*-aminophenol of about 1500 cm^{-1} at the B3LYP/6-311++G-(2d,2p) level of theory. Therefore, conversion from cis to trans is unlikely for our experimental conditions.

NH-Stretching Vibrations. The detailed overtone spectra of the regions corresponding to $\Delta v_{\mathrm{NH}} = 2$ and 3 are shown in Figures 3 and 4, respectively. The observed and calculated NH-stretching band positions are presented in Table 4, in which we also compare to previous results for aniline.[10,27] The observed fundamental transitions are included in Table 4.

In the $\Delta v_{\mathrm{NH}} = 2$ region of the jet-cooled aniline spectrum,[10] three strong bands are observed and assigned to the $|20\rangle_{+}$, $|20\rangle_{-}$, and $|11\rangle$ local mode states ($2\nu_{\mathrm{s}}$, $\nu_{\mathrm{s}} + \nu_{\mathrm{as}}$, and $2\nu_{\mathrm{as}}$ normal modes). Two weaker peaks at lower energy are assigned to stretch−bend combinations resonance-coupled to the $\Delta v_{\mathrm{NH}} = 2$ stretching states.[10] The spectra of the three aminophenols, shown in Figure 3, closely resemble that of aniline. The NH-stretching transitions in *o*- and *m*-aminophenol appear at very similar energies, while in *p*-aminophenol these transitions are situated at significantly lower energy, in agreement with the calculated bond lengths in Table 2. The absolute agreement between observed and calculated transition wavenumbers is only reasonable in this region, due to the neglect of resonance coupling in our theoretical model.

For *p*-aminophenol, the observed intensity ratio of the three main NH-stretching transitions in the $\Delta v_{\mathrm{NH}} = 2$ region is 1:0.39:0.14. The calculated relative intensities of the three main peaks are similar in each aminophenol, and for *p*-aminophenol the ratio is 1:0.53:0.08, which is in good agreement with the observed relative intensities. Because of changes in laser power, a comparison of intensities from the NID spectra should only be made over a small energy range.

In the *m*-aminophenol spectrum, the $|20\rangle_{+}$, $|20\rangle_{-}$, and $|11\rangle$ transitions from both the trans conformer and the less abundant cis conformer are clearly visible. The separation of the trans

TABLE 4: Observed and Calculated NH-Stretching Frequencies (in cm^{-1})

	o-aminophenol (trans)		*m*-aminophenol				*p*-aminophenol		aniline	
			cis		trans					
state	obsd	calcd[a]	obsd	calcd[a]	obsd	calcd[a]	obsd	calcd[a]	obsd	calcd[b]
$\|10\rangle_+$	3425	3423	3428	3422	3428	3424	3405[c]	3408	3420.9[d]	3420
$\|10\rangle_-$	3518	3516	3517	3509	3517	3514	3488[c]	3493	3508.2[d]	3507
$\|20\rangle_+$	6743	6733	6741	6730	6749	6735	6709	6702	6738.0[e]	6726
$\|20\rangle_-$	6789	6776	6782	6768	6790	6775	6746	6738	6778.7[e]	6764
$\|11\rangle$	6963	6981	6949	6969	6960	6977	6909	6938	6947.6[e]	6965
$\|30\rangle_+$		9894	9870	9884	9883	9894	9822	9840	9873[b]	9879
$\|30\rangle_-$		9905		9894	9897	9904		9848	9889[b]	9887

[a] Calculated with the local mode parameters in Table 1. [b] Taken from ref 27, calculated with experimental local mode parameters and measured at room temperature. [c] Taken from ref 16. Reference 15 reported values of 3407 and 3492 cm^{-1}. [d] Taken from ref 26. [e] Taken from ref 10.

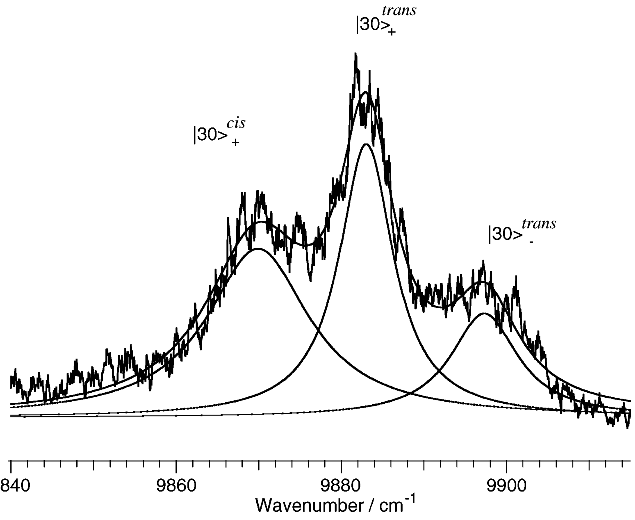

Figure 8. NID spectra of jet-cooled *m*-aminophenol in the $\Delta v_{NH} = 3$ region.

TABLE 5: Calculated Total OH- and NH-Stretching Oscillator Strengths[a]

	o-aminophenol (trans)		*m*-aminophenol				*p*-aminophenol		
			cis		trans				
v	OH	NH	OH	NH	OH	NH	OH	NH	exponent
1	8.7	5.7	6.8	3.1	8.2	3.5	7.6	2.1	10^{-6}
2	6.9	7.8	6.8	7.7	7.2	7.7	7.3	8.5	10^{-7}
3	3.4	3.0	3.7	3.2	3.8	3.2	3.9	3.4	10^{-8}
4	1.8	1.6	2.1	1.7	2.1	1.7	2.2	2.0	10^{-9}

[a] Calculated with the local mode parameters in Table 1 and B3LYP/6-311++G(2d,2p) DMFs.

and cis NH-stretching peaks is about 10 cm^{-1} in this region, which is larger than the 2 cm^{-1} separation of the OH-stretching peaks.

In the spectrum of *o*-aminophenol, two bands of reasonable strength at 6713 and 6913 cm^{-1} could not be assigned to the trans conformer. These observations led us to consider the existence of a cis isomer, which we will discuss in the following section.

Transitions corresponding to $\Delta v_{NH} = 3$ are clearly identified in the spectra of *p*-aminophenol and *m*-aminophenol, as shown in Figure 4. For *p*-aminophenol we assign the strong peak at 9822 cm^{-1} to the $|30\rangle_+$ transition, and the calculated wavenumber is within 20 cm^{-1} of the observed value. An expanded version of the $\Delta v_{NH} = 3$ region of the *m*-aminophenol spectrum is shown in Figure 8. We have assigned the strongest band at 9883 cm^{-1} to the $|30\rangle_+$ transition in the trans conformer, and the weaker band at 9897 cm^{-1} to the $|30\rangle_-$ transition. Our calculations predict the intensity of the $|30\rangle_+$ transition to be roughly twice that of the $|30\rangle_-$ transition, and the separation of the transitions to be about 10 cm^{-1}. The corresponding transitions in the cis conformer are predicted to be situated about 10 cm^{-1} lower in energy than those of the trans conformer. We assign the lowest energy band at 9870 cm^{-1} to the $|30\rangle_+$ transition in the cis isomer, while the less intense $|30\rangle_-$ transition is expected to lie in the region of the trans peaks and is obscured.

The total OH- and NH-stretching intensities calculated with our anharmonic oscillator model are shown in Table 5. For the fundamental region, the results can be compared to the OH to NH relative intensity ratios determined from gas-phase infrared spectra from the NIST Standard Reference Database.[37] The calculated OH to NH intensity ratios increase in the order *o*- < *m*- < *p*-aminophenol, which is in agreement with the gas-phase data. For *p*-aminophenol we calculate the OH-stretching intensity to be about 3 times stronger than the total NH-stretching intensity, which is close to the ratio of 2.6:1 determined from the NIST data, as well as in qualitative agreement with published NID spectra.[15,16]

In all aminophenols, the calculated ratio of OH- to NH-stretching intensity in the $\Delta v_{NH} = 3$ region is close to 1:0.9. For *m*- and *p*-aminophenol the observed relative intensities from the NID spectra are close to unity, in good agreement with our calculations. It is thus somewhat surprising that NH-stretching transitions are not clearly observed in the $\Delta v_{NH} = 3$ spectrum of *o*-aminophenol.

Intramolecular Hydrogen Bonding in *o*-Aminophenol. The NID spectra of jet-cooled *o*-aminophenol in the fundamental and first overtone regions are shown in Figures 6 and 3, respectively. We observed four bands, at 3480, 3605, 6715, and 6913 cm^{-1}, that could not readily be assigned to the trans conformer. To investigate the origin of the IR transitions we recorded an IR-dip spectrum of *o*-aminophenol. In the IR-dip spectrum the frequency of the UV laser was fixed to 33 700 cm^{-1}, corresponding to a vibronic transition in *o*-aminophenol. The IR-dip spectrum, shown in Figure 6, demonstrates that the three strongest bands observed in the NID-IR spectrum at 3425, 3518, and 3666 cm^{-1} originate from one species, while the weaker bands at 3480 and 3610 cm^{-1} must arise from another species.

An explanation for the anomalous bands could be the possible existence of a cis conformer. For steric reasons, a cis conformer can only be accommodated by a rotation of the NH_2 group out of the plane of the aromatic ring. The cis conformer, shown in Figure 1, is characterized by its C_s symmetry and an OH$\cdots$N intramolecular hydrogen bond. Recently, Korth et al.[38] used DFT calculations with the B3LYP/6-31G(d,p) method to study intramolecular hydrogen bonding in a range of ortho-substituted phenols. The trans and cis conformers were both found to be stable minima in the B3LYP/6-31G(d,p) optimizations, with the cis conformer lower in energy by 0.4 kcal mol^{-1}. Their results are, however, inconsistent with the solution-phase infrared spectrum of *o*-aminophenol,[17,19,39] which shows no evidence for intramolecular OH···N hydrogen-bonding interaction, but rather exhibits an OH-stretching transition frequency essentially indistinguishable from that of *p*-aminophenol or bare phenol.

In agreement with the solution phase observations and our present spectra recorded in the collision-free environment of the supersonic jet, our B3LYP/6-311++G(2d,2p) and MP2/6-311++G(2d,2p) calculations predict the trans conformer as the lowest energy structure. The cis conformer is found to have one imaginary frequency and an energy (B3LYP) that is 0.6 kcal mol^{-1} higher than the trans conformer. The imaginary frequency corresponds to simultaneous rotation of the hydroxyl and amino groups about the CO and CN bonds, respectively, toward the trans orientation.

If one was to assume hypothetically the existence of the cis conformer, then the feature at 3480 cm^{-1} could correspond to its OH-stretching fundamental vibration. This band is about one-third the intensity of the trans OH-stretching band. Our anharmonic oscillator intensity calculations predict that the OH-stretching transition in the cis conformer is about three times the strength of that in the trans conformer, and thus the population of the cis conformer would have to be very small.

It is possible that the small bands at 3350 and 3440 cm^{-1} in the *o*-aminophenol NID spectrum could be NH-stretching vibrations in the cis conformer. These transitions are calculated to be about half the strength of those in the trans conformer, which means that the cis conformer would have to be reasonably abundant. This contradicts the results from the OH-stretching region. Furthermore, in the $\Delta\upsilon_{NH} = 2$ region the NH-stretching transition of the cis conformer is predicted to have an intensity approximately twice that of the trans conformer NH-stretch and would be located around 6570 cm^{-1}. We do not observe any peaks in this region. The spectral evidence for the cis conformer of *o*-aminophenol is thus inconclusive and we think it is more likely that the unassigned peaks are due to contamination from other species.

To gain a better understanding of electronic effects in *o*-aminophenol we have performed natural bond orbital (NBO) analyses using the B3LYP/6-311++G(2d,2p) calculated density matrixes. In both conformers of *o*-aminophenol delocalization of electron density from the π-bonding NBOs into the π*-antibonding NBOs results in strong π resonance, typical of aromatic systems.[40]

In *trans*-*o*-aminophenol the amino group adopts an aniline-like geometry, which allows for maximum resonance stabilization between the nitrogen lone pair and the π* NBOs of the ring. The nitrogen lone pair has 88% *p* character and an occupancy of 1.85, which indicates strong delocalization of electron density from the limiting value of 2 for a completely localized electron pair. Second-order perturbation theory estimates an energetic stabilization of 25 kcal mol^{-1} from the lone pair to π* interaction. Removal of the lone pair to π* interaction by the deletion of orbitals leads to an energy increase of 23 kcal mol^{-1}, in good agreement with the prediction from perturbation theory.

The formation of a strong intramolecular hydrogen bond would be characterized by a significant delocalization of electron density from the lone pair on the acceptor atom to the σ* orbital on the donor, as has been seen for example in the NBO analysis of the water dimer.[41] A perturbative analysis of the NH···O hydrogen bond in *trans*-*o*-aminophenol predicts that the interaction between the oxygen lone pair and NH$_t$ σ* NBO gives less than 0.5 kcal mol^{-1} of stabilization energy, indicating a very weak hydrogen bond.

In the cis conformer, the nitrogen lone pair has somewhat less *p* character (83%), and because it is located in the plane of the benzene ring, the π* resonance stabilization is lost. The nitrogen lone pair is significantly more localized (1.95) and the stabilization interaction from the lone pair to the σ* NBOs of the ring is only about 12 kcal mol^{-1}. Perturbation theory analysis shows that the formation of a relatively strong OH···N hydrogen bond in *cis*-*o*-aminophenol leads to an energy stabilization of about 5 kcal mol^{-1} from nitrogen lone pair to OH σ* NBO delocalization.

The B3LYP/6-311++G(2d,2p) calculated energy of *trans*-*o*-aminophenol is 0.6 kcal mol^{-1} lower than that of the cis conformer. The significant driving force that favors the trans conformer is the strong π-donation from the amino group to the ring, which cannot be offset by the formation of a relatively strong OH···N hydrogen bond in the cis conformer.

Conclusion

We have presented a method to probe rotational isomers based on vibrational overtone spectroscopy of jet-cooled molecules. In jet-cooled *m*-aminophenol, the OH-stretching transitions of cis and trans conformers are clearly resolved and assigned in the vibrational overtone spectra, despite a difference in bond lengths of only about 0.02 mÅ. The energy difference between the two conformers calculated by using density functional theory is in reasonable agreement with the observed relative intensities. These results show that overtone spectroscopy of jet-cooled molecules combined with local mode calculations of vibrational energies and intensities can be used as a tool for distinguishing between closely related rotational isomers.

We assign the vibrational spectrum of *o*-aminophenol to the trans species, in agreement with our ab initio and anharmonic vibrational calculations. We do not observe clear evidence for the existence of a *cis*-*o*-aminophenol rotational isomer.

Acknowledgment. The authors would like to thank Daryl L. Howard for helpful discussions. M.F. would like to thank the Lasers and Applications Research Theme at the University of Otago for providing travel funds for a visit. H.G.K. is grateful to the Japan Society for Promotion of Science for a visiting fellowship, and T.W.R. is grateful to the Foundation for Research, Science and Technology for a Bright Futures Top Achiever Doctoral Scholarship. The Ministry of Education, Culture, Sports, Science and Technology (MEXT), the Marsden Fund administered by the Royal Society of New Zealand, and the University of Otago have provided funding for this research.

Supporting Information Available: One table with B3LYP/6-311++G(2d,2p) calculated harmonic frequencies and intensities of the aminophenol structures shown in Figure 1. This material is available free of charge via the Internet at http://pubs.acs.org.

References and Notes

(1) Weinkauf, R.; Schermann, J.-P.; de Vries, M. S.; Kleinermanns, K. *Eur. Phys. J. D* **2002**, *20*, 309.

(2) Robertson, E. G.; Simons, J. P. *Phys. Chem. Chem. Phys.* **2001**, *3*, 1.

(3) Johnson, J. R.; Jordan, K. D.; Plusquellic, D. F.; Pratt, D. W. *J. Chem. Phys.* **1990**, *93*, 2258.

(4) Oikawa, A.; Abe, H.; Mikami, N.; Ito, M. *Chem. Phys. Lett.* **1985**, *116*, 50.

(5) Oikawa, A.; Abe, H.; Mikami, N.; Ito, M. *J. Phys. Chem.* **1984**, *88*, 5180.

(6) Suzuki, K.; Emura, Y.; Ishiuchi, S.; Fujii, M. *J. Electron Spectrosc. Relat. Phenom.* **2000**, *108*, 13.

(7) Henry, B. R. *Acc. Chem. Res.* **1987**, *20*, 429.

(8) Levy, D. H. *Annu. Rev. Phys. Chem.* **1980**, *31*, 197.

(9) Ishiuchi, S.; Shitomi, H.; Takazawa, K.; Fujii, M. *Chem. Phys. Lett.* **1998**, *283*, 243.

(10) Fehrensen, B.; Hippler, M.; Quack, M. *Chem. Phys. Lett.* **1998**, *298*, 320.

(11) Kjaergaard, H. G.; Henry, B. R. *J. Phys. Chem.* **1995**, *99*, 899.

(12) Kjaergaard, H. G.; Howard, D. L.; Schofield, D. P.; Robinson, T. W.; Ishiuchi, S.; Fujii, M. *J. Phys. Chem. A* **2002**, *106*, 258.

(13) Shinozaki, M.; Sakai, M.; Yamaguchi, S.; Fujioka, T.; Fujii, M. *Phys. Chem. Chem. Phys.* **2003**, *5*, 5044.

(14) Reese, J. B.; Pratt, D. W. Unpublished work.

(15) Gerhards, M.; Unterberg, C. *Appl. Phys. A* **2001**, *72*, 273.

(16) Mori, H.; Kugisaki, H.; Inokuchi, Y.; Nishi, N.; Miyoshi, E.; Sakota, K.; Ohashi, K.; Sekiya, H. *Chem. Phys.* **2002**, *277*, 105.

(17) Agashe, M. S.; Jose, C. I. *J. Chem. Soc., Faraday Trans. 2* **1977**, *73*, 1227.

(18) Griffith, W. P.; Koh, T. Y. *Spectrochim. Acta* **1995**, *51A*, 253.

(19) Krueger, P. J. *Tetrahedron* **1970**, *26*, 4753.

(20) Mortensen, O. S.; Henry, B. R.; Mohammadi, M. A. *J. Chem. Phys.* **1981**, *75*, 4800.

(21) Child, M. S.; Halonen, L. *Adv. Chem. Phys.* **1984**, *57*, 1.

(22) Kjaergaard, H. G.; Yu, H.; Schattka, B. J.; Henry, B. R.; Tarr, A. W. *J. Chem. Phys.* **1990**, *93*, 6239.

(23) Kjaergaard, H. G.; Turnbull, D. M.; Henry, B. R. *J. Chem. Phys.* **1993**, *99*, 9438.

(24) Davidsson, J.; Gutow, J. H.; Zare, R. N. *J. Phys. Chem.* **1990**, *94*, 4069.

(25) Omi, T.; Shitomi, H.; Sekiya, N.; Takazawa, K.; Fujii, M. *Chem. Phys. Lett.* **1996**, *252*, 287.

(26) Fehrensen, B.; Luckhaus, D.; Quack, M. *Z. Phys. Chem.* **1999**, *209*, 1.

(27) Howard, D. L.; Robinson, T. W.; Fraser, A.; Kjaergaard, H. G. *Phys. Chem. Chem. Phys.* **2004**, *6*, 719.

(28) Ebata, T. Population Labelling Spectroscopy. In *Nonlinear Spectroscopy for Molecular Structure Determination*; Field, R. W., Hirota, E., Maier, J. P., Tsuchiya, S., Eds.; Blackwell: Oxford, UK, 1998; p 149.

(29) Atkins, P. W.; Friedman, R. S. *Molecular Quantum Mechanics*, 3rd ed.; Oxford University Press: Oxford, UK, 1997.

(30) Kjaergaard, H. G.; Goddard, J. D.; Henry, B. R. *J. Chem. Phys.* **1991**, *95*, 5556.

(31) Sowa, M. G.; Henry, B. R.; Mizugai, Y. *J. Phys. Chem.* **1991**, *95*, 7659.

(32) Low, G. R.; Kjaergaard, H. G. *J. Chem. Phys.* **1999**, *110*, 9104.

(33) Reddy, K. V.; Heller, D. F.; Berry, M. J. *J. Chem. Phys.* **1982**, *76*, 2814.

(34) Glendening, E. D.; Reed, A. E.; Carpenter, J. E.; Weinhold, F. NBO Version 3.1.

(35) Frisch, M. J.; Trucks, G. W.; Schlegel, H. B.; Scuseria, G. E.; Robb, M. A.; Cheeseman, J. R.; Zakrzewski, V. G.; Montgomery, J. A.; Stratmann, R. E.; Burant, J. C.; Dapprich, S.; Millam, J. M.; Daniels, A. D.; Kudin, K. N.; Strain, M. C.; Farkas, O.; Tomasi, J.; Barone, V.; Cossi, M.; Cammi, R.; Mennucci, B.; Pomelli, C.; Adamo, C.; Clifford, S.; Ochterski, J.; Petersson, G. A.; Ayala, P. Y.; Cui, Q.; Morokuma, K.; Malick, D. K.; Rabuck, A. D.; Raghavachari, K.; Foresman, J. B.; Cioslowski, J.; Ortiz, J. V.; Baboul, A. G.; Stefanov, B. B.; Liu, G.; Liashenko, A.; Piskorz, P.; Komaromi, I.; Gomperts, R.; Martin, R. L.; Fox, D. J.; Keith, T.; Al-Laham, M. A.; Peng, C. Y.; Nanayakkara, A.; Gonzalez, C.; Challacombe, M.; Gill, P. M. W.; Johnson, B.; Chen, W.; Wong, M. W.; Andres, J. L.; Head-Gordon, M.; Replogle, E. S.; Pople, J. A. *Gaussian 98*, Revision A.7; Gaussian, Inc.: Pittsburgh, PA, 1998.

(36) Ruoff, R. S.; Klots, T. D.; Emilsson, T.; Gutowsky, H. S. *J. Chem. Phys.* **1990**, *93*, 3142.

(37) *NIST Chemistry WebBook, NIST Standard Reference Database Number 69*; Linstrom, P. J., Mallard, W. G., Eds.; National Institute of Standards and Technology: Gaithersburg, MD, 2003 (http: //webbook.nist.gov).

(38) Korth, H.-G.; de Heer, M. I.; Mulder, P. *J. Phys. Chem. A* **2002**, *106*, 8779.

(39) Musso, H.; Sandrock, G. *Chem. Ber.* **1964**, *97*, 2076.

(40) Reed, A. E.; Weinhold, F. *J. Chem. Phys.* **1985**, *83*, 1736.

(41) Reed, A. E.; Curtiss, L. A.; Weinhold, F. *Chem. Rev.* **1988**, *88*, 899.